Ab-initio and DFT Study of the Molecular Mechanisms of SO₃ and SOCl₂ Reactions with Water in the Gas Phase

Stanislav K. Ignatov*

Alfred Wegener Institute for Polar- und Marine Research, Bremerhaven, Germany, and University of Nizhny Novgorod, Nizhny Novgorod, Russia

Petr G. Sennikov[†]

Alfred Wegener Institute for Polar- und Marine Research, Bremerhaven, Germany, and Institute of High-Pure Substances of RAS, Nizhny Novgorod, Russia

Alexey G. Razuvaev[‡]

University of Nizhny Novgorod, Nizhny Novgorod, Russia

Otto Schrems[§]

Alfred Wegener Institute for Polar- und Marine Research, Bremerhaven, Germany

The molecular reaction pathways of SO_3 and $SOCl_2$ reactions with one and two water molecules were studied using ab-initio and DFT quantum chemical methods (up to MP2/6-311++G(3df,3pd) and QCISD(T)/6-311++G(2df,2pd)) in order to describe the experimentally observed kinetic features of SO_3 hydration and $SOCl_2$ hydrolysis in the gas phase and to elucidate the reaction mechanism providing the high reaction rate. The transition state structures were located, and absolute values of kinetic rate constants were estimated for a variety of possible reaction pathways including bi- and termolecular S=O and S−Cl bond hydrolysis, chlorine shift to oxygen, dissociative addition with formation of hexavalent sulfur derivative, and adjacent reactions. It was found that the termolecular mechanism of SO_3 hydration proposed earlier by Morokuma and Muguruma is in good agreement with the experimental rate constants. However, none of the proposed molecular pathways of $SOCl_2$ hydrolysis can provide the high reaction rate observed experimentally. Thus, the real hydrolysis mechanism of halogen derivatives of second-row elements in the gas phase can be sufficiently different from the regular molecular pathways, which are usually considered.

Introduction

The gas-phase hydrolysis and hydration reactions of sulfur-containing species in the Earth atmosphere, forming sulfur oxides and halogenides, are among the key processes that contribute to environmental pollution such as acid rain and related phenomena. From this point of view, gas-phase kinetic studies of the sulfur oxides and halogenides are important for a better understanding of the atmospheric reactions of these species. Surprisingly, there were incomplete or controversial experimental measurements on the SO_3 hydration kinetics and a lack of direct experimental data on the kinetic feature of $SOCl_2$ hydrolysis up to the last decade. The development of sophisticated experimental techniques in recent years, above all the turbulent-flow technique,[1] made it possible to determine directly the reaction orders and rate constants for the gas-phase reactions of SO_3. It was found[2−4] that the gas-phase SO_3 hydration is a second-order reaction for water, not first-order as it was reported

earlier,[5−8] occurring with a rather high rate of 3.1×10^{-31} (ref 4) or 2.3×10^{-31} cm⁶ molecule⁻² s⁻¹ (ref 3) at 298 K. It should be noted that particular attention has been paid in thorough studies[3,4] to eliminate the effects of heterogeneous reactions proceeding on walls, drops, and other surfaces. As a result, it was possible to estimate the contribution of heterogeneous reactions to the whole reaction rate.[3] Thus, the above rate constant values are parameters characterizing the truly gas-phase reactions. Recently, the reaction kinetics of $SOCl_2$ hydrolysis was studied by gas-phase IR spectroscopy in a high-volume chamber, and it was found that the reaction is of first order for both $SOCl_2$ and water.[9] The bimolecular reaction rate was reported to be 6.3×10^{-21} cm³ molecule⁻¹ s⁻¹ at 297 K.[9]

These relatively high reaction rates imply that the reaction barriers of the hydration and hydrolysis processes are low. However, it was found already in the earlier quantum chemical studies[10,11] that the activation energy of SO_3 hydration is about 100 kJ mol⁻¹, making a fast bimolecular reaction in the gas-phase impossible. To explain the high reaction rate of SO_3 hydration, Morokuma and Muguruma[12] proposed that this reaction proceeds through the termolecular transition state SO_3·$(H_2O)_2$. The coordination of an additional water molecule leads to a crucial decrease of the activation barrier and is in agreement

* Corresponding author. Stanislav K. Ignatov, Spectroscopy Chair, Department of Chemistry, University of Nizhny Novgorod, 23 Gagarin Avenue, Nizhny Novgorod 603600, Russia. E-mail: ignatov@ichem.unn.runnet.ru.
  † E-mail: sen@ihps.nnov.ru.
  ‡ E-mail: tcg@ichem.unn.runnet.ru.
  § E-mail: oschrems@awi-bremerhaven.de.

with the second-order kinetics for water observed experimentally. However, there was no direct comparison with an experimental rate constant (because the accurate experimental data was not available). It should be noted that the idea of speeding up the gas-phase reactions by coordinating several water molecules to the transition state is very attractive to explain the kinetic features of various processes. It was used, for example, in studies by Vincent et al.[13] to explain the fast gas-phase reactions between SO_2 and H_2O_2, in a series of investigations by Kudo and Gordon[14,15] on the Si−Hal and Si−C hydrolysis (regarding to the liquid-phase reaction), Ignatyev et al.,[16] Okumoto et al.[17] (Si−C bond hydrolysis), Lewis and Glaser[18] (CO_2 hydration), and others. However, in all these studies there was no direct comparison with experimentally measured rate constants, and the conclusions made on the basis of the multimolecular mechanism were limited only by the qualitative description leading to the statement about significant lowering of the activation barrier due to the coordination. Recently, we have undertaken an attempt to calculate the rate constant of the gas-phase $SiCl_4$ hydrolysis using the conventional transition state theory and the G2(MP2) method for the estimation of accurate activation energy for bi-, ter-, and tetramolecular transition states located at the B3LYP level.[19] Surprisingly, although the calculated rate constant was in very good agreement with the experimental data in the high-temperature region (where the simple bimolecular kinetics was found), it was typically 6 or 7 orders of magnitude lower than the experimental values in the low-temperature region where the second order for water and the negative apparent activation energy were observed.[20,21]

Thus, the interesting question arises as to whether the proposals about the bi- or multimolecular mechanisms of S−Cl bond hydrolysis agree with the available data on the direct gas-phase kinetics of $SOCl_2$ and, more generally, what is the mechanism of the gas-phase reactions of these species with water. Since the SO_3 hydration kinetics is considered by us as the most reliable data to date (it was studied recently by two independent groups, and their results were in good agreement), it is reasonable to use these data as an additional reference point to validate the calculations on the $SOCl_2$ system and, additionally, to make a direct validation (by comparison between the experimental and calculated rate constant) for the termolecular mechanism proposed by Morokuma.[12] It is also interesting to compare the results on the gas-phase S−Cl bond hydrolysis with the previous results on the low-temperature hydrolysis mechanism of silicon halogenides which is not yet understood. As to applications, the mechanistic study can provide additional information for some important reactions of sulfur-containing species relevant in atmospheric modeling.

Calculation Details

All the calculations were performed using the Gaussian98[22] program suite. The stationary points were located using the DFT (B3LYP) and MP2 methods with further improvement of energy at the CCSD(T) and QCISD(T) levels. Various basis sets were examined up to 6-311++G(3df,3pd) and aug-cc-pVTZ. For brevity, we will use hereafter the shortened notation for four most frequently used basis sets: 3df (for 6-311++G(3df,3pd)), 2df (for 6-311++G(2df,2pd)), 2d (for 6-311++G(2d,2p)), and VDZ (for aug-cc-pVDZ). The G3[23] method was used for high-accuracy calculations of reactions enthalpies. All the transition structures were located without any constraints by Berny's and QST2 methods implemented in Gaussian98 and were characterized by frequency calculations. The rigid rotor−harmonic

oscillator (RRHO) approximation was used for calculations of partition functions. In some critical cases, the effect of internal rotations on the Gibbs free energy and partition functions was examined using the Pitzer-Gwinn approach[24] as it is implemented in MOLTRAN program.[25] The conventional transition state theory (TST) was used for the calculation of rate constants.
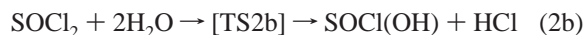
Proposed Mechanisms

The SO_3 hydration and $SOCl_2$ hydrolysis can be presented by the following equations:

$$SO_3 + H_2O \rightarrow H_2SO_4 \tag{1}$$

$$SOCl_2 + H_2O \rightarrow SO_2 + 2HCl \tag{2}$$
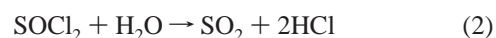
As shown in ref 12, the significant decrease of the activation barrier for reaction 1 takes place when the additional water molecule is coordinated to the regular four-membered transition state TS1a, forming the termolecular transition state TS1b where two water molecules form the six-membered [···S−O···H−O(H)···H−O(H)···] ring together with breaking the S=O bond. Thus, reaction 1 can then be presented by two possible pathways:

$$SO_3 + H_2O \rightarrow [TS1a] \rightarrow H_2SO_4 \tag{1a}$$

$$SO_3 + 2H_2O \rightarrow [TS1b] \rightarrow H_2SO_4 + H_2O \tag{1b}$$
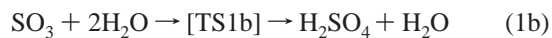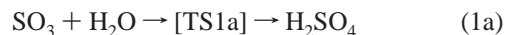
Analogously, we propose similar schemes for the initial step of the $SOCl_2$ hydrolysis:

$$SOCl_2 + H_2O \rightarrow [TS2a] \rightarrow SOCl(OH) + HCl \tag{2a}$$

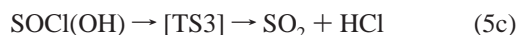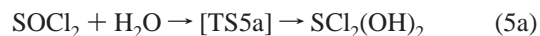$$SOCl_2 + 2H_2O \rightarrow [TS2b] \rightarrow SOCl(OH) + HCl \tag{2b}$$

The next step of mechanisms (eqs 2a and 2b) is an elimination of HCl from the formed SOCl(OH) through the corresponding transition state TS3:

$$SOCl(OH) \rightarrow [TS3] \rightarrow SO_2 + HCl \tag{3}$$
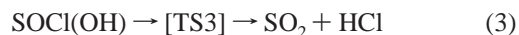
In addition to mechanism 2a, we examined the concerted mechanism of simultaneous hydrolysis of two S−Cl bonds occurring in a one-step reaction through the transition state TS4:

$$SOCl_2 + H_2O \rightarrow [TS4] \rightarrow SO_2 + 2HCl \tag{4}$$
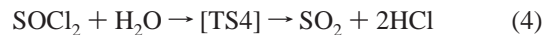
The hydrolysis process can also involve the S=O bond hydration with subsequent two-step HCl elimination from an intermediate:

$$SOCl_2 + H_2O \rightarrow [TS5a] \rightarrow SCl_2(OH)_2 \tag{5a}$$

$$SCl_2(OH)_2 \rightarrow [TS6] \rightarrow SOCl(OH) + HCl \tag{5b}$$

$$SOCl(OH) \rightarrow [TS3] \rightarrow SO_2 + HCl \tag{5c}$$

Like the S−Cl hydrolysis, reaction 5a can proceed also through the termolecular transition state with an additionally coordinated water molecule:

$$SOCl_2 + 2H_2O \rightarrow [TS5b] \rightarrow SCl_2(OH)_2 + H_2O \tag{5d}$$
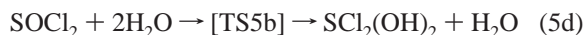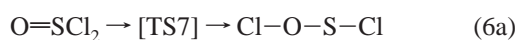
It cannot be excluded, however, that the hydrolysis occurs through the monomolecular (rate-determining) step of $SOCl_2$ rearrangement with further hydrolysis of the O−Cl bond in the

TABLE 1: Calculated Energies (E_{tot}) and Imaginary Frequencies (ν_{im}) of Transition States, Kinetic Parameters, and Rate Constants (k) of SO$_3$ Hydration

reaction	E_{tot} a.u.	ν_{im} cm^{-1}	$E_a{}^a$ kJ mol^{-1}	$\Delta H_0{}^{\neq b}$ kJ mol^{-1}	$\Delta G^{\neq c}$ kJ mol^{-1}	k cm^3 molecule^{-1} s^{-1} [cm^6 molecule^{-2} s^{-1}]^d
SO$_3$ + H$_2$O → [TS1a] → H$_2$SO$_4$						
B3LYP/2d	−700.3316100	1654i	81.0	83.6	121.0	1.6 (−28) [3.2 (−46)]
B3LYP/3df	−700.3722203	1633i	74.3	76.8	118.7	4.0 (−28) [8.0 (−46)]
MP2/VDZ	−699.0140075		81.1	(83.6)^e	(125.5)^e	2.6 (−29) [5.2 (−47)]
MP2/2df	−699.3189954		67.7	(63.3)	(112.2)	5.7 (−27) [1.1 (−44)]

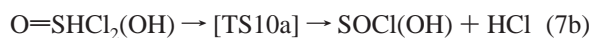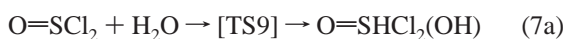| reaction	E_{tot} a.u.	ν_{im} cm^{-1}	$E_a{}^a$ kJ mol^{-1}	$\Delta H_0{}^{\neq b}$ kJ mol^{-1}	$\Delta G^{\neq c}$ kJ mol^{-1}	k cm^6 molecule^{-2} s^{-1}
SO$_3$ + 2H$_2$O → [TS1b] → H$_2$SO$_4$ + H$_2$O						
B3LYP/2d	−776.8377131	637i	−34.7	−18.6	62.1	1.4 (−37)
B3LYP/3df	−776.8823413	643i	−44.6	−28.8	47.3	4.8 (−35)
MP2/VDZ	−775.3182221		−32.6	(−16.8)^e	(59.3)^e	3.9 (−37)
MP2/2df	−775.6860332		−56.2	(−40.4)^e	(35.7)^e	5.0 (−33)
MP2/3df//B3LYP/3df	−775.7190718		−55.0	(−39.2)^e	(36.9)^e	3.0 (−33)
CCSD(T)/VDZ//MP2/VDZ	−775.3669998		−35.5	(−19.7)^e	(56.4)^e	1.2 (−36)
experiment^{3,4}						2.3 (−31), 3.1 (−31)

^{a} Activation energy. ^{b} Zero-temperature enthalpy of activation $\Delta H_0{}^{\neq} = E_a +$ ZPE. ^{c} Standard Gibbs free energy of activation. ^{d} The values in square brackets are "effective termolecular constants" k_{III} converted from bimolecular rate constants by formula $k_{III} = k_{II}/[H_2O]$ (where [H$_2$O] = 5 × 10^{17} molecules/cm^3—typical experimental concentrations of water). Only k_{III} can be directly compared with experimental values for SO$_3$ hydration. ^{e} Calculated on the basis of the B3LYP/3df frequencies and geometry parameters.

Cl−O−S−Cl intermediate:

$$O{=}SCl_2 \rightarrow [TS7] \rightarrow Cl{-}O{-}S{-}Cl \qquad (6a)$$

$$Cl{-}O{-}S{-}Cl + H_2O \rightarrow [TS8] \rightarrow HCl + SOCl(OH) \qquad (6b)$$

Formed SOCl(OH) then undergoes further rearrangement in agreement with reaction 3.

Because it is quite typical for sulfur to form hexavalent compounds, an additional pathway of dissociative addition of H$_2$O to SOCl$_2$ resulting in the hexavalent derivative O=SHCl$_2$-(OH) undergoing further transformations to SOCl(OH) or SCl$_2$-(OH)$_2$ was also considered:

$$O{=}SCl_2 + H_2O \rightarrow [TS9] \rightarrow O{=}SHCl_2(OH) \qquad (7a)$$

$$O{=}SHCl_2(OH) \rightarrow [TS10a] \rightarrow SOCl(OH) + HCl \qquad (7b)$$

$$O{=}SHCl_2(OH) \rightarrow [TS10b] \rightarrow SCl_2(OH)_2 \qquad (7c)$$

Although not all of the equations 2−7 correspond to the experimentally observed first-order kinetics for water,^{9} it seems to be reasonable to consider all the above reactions because the experimental determination of reaction order can be influenced by various effects (and the apparent value of order can be significantly different from the true one).

Calculation Results

SO$_3$ Hydration. To give the correct description of the SO$_3$ hydration, the source reagents SO$_3$ and H$_2$O and the transition states TS1a and TS1b were calculated using the extended basis sets and the modern methods for better correlation treatment and the geometries of ref 12 as starting points. The B3LYP and MP2 methods were used for optimization with further specification of transition state energies at the QCISD(T) and CCSD(T) levels. The optimized geometries are shown in Figure 1 (the geometry parameters of source SO$_3$ and H$_2$O calculated at the B3LYP/3df and MP2/2df (in parentheses) levels are the following: r(S−O), Å = 1.425(1.429); r(O−H), Å = 0.961-(0.959); ∠HOH, degrees = 105.1(104.1)). The calculated thermodynamic and kinetic parameters of reactions 1a and 1b
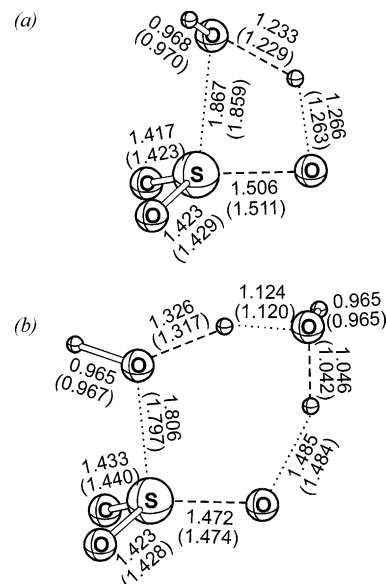

Figure 1. B3LYP/3df and MP2/2df (in parentheses) optimized structural parameters of transition states of SO$_3$ hydration: (a) TS1a; (b) TS1b. Hereafter, the dashed line marks a formed bond; the dotted line a breaking bond.

are presented in Table 1. As follows from the Table 1, the activation barrier of reaction 1a is too high to explain the fast bimolecular reaction measured.$^{10-12}$ For reaction 1b, the modest levels of theory yield the unrealistically high activation barrier. However, the improvement of the theoretical level has a large effect on the calculated rate constant value. Figure 2 shows the temperature dependence of calculated rate constants for reaction 1b calculated at the various levels of theory. As follows from Figure 2, the B3LYP/2d and MP2/2d results are typically 5 or 6 orders of magnitude lower than the experimental values. The use of 2df and 3df basis sets has a noticeable effect on the calculated rate constants, increasing their values. The MP2 values are typically better than the B3LYP results. The QCISD-(T) and CCSD(T) corrections have a little back-effect lowering the calculated rates. The best results have been obtained at the MP2/6-311++G(3df,2pd)//B3LYP/6-311++G(3df,2pd) and
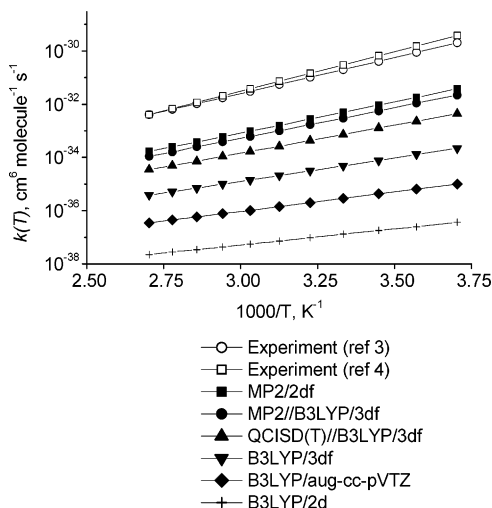
Mechanisms of SO₃ and SOCl₂ Reactions with Water

J. Phys. Chem. A, Vol. 108, No. 16, 2004 **3645**

Figure 2. Comparison between the experimental and calculated rate constants of the gas-phase hydration of SO₃ (termolecular reaction 1b).

MP2/2df levels. In these cases, the calculated values are lower than the experimental ones, typically by 2 orders of magnitude. It is believed that further improving the quantum chemical level will not lead to the reduction of this discrepancy. Most likely, the discrepancy has two origins. First, the hydrogen tunneling should be important in this reaction. It can increase the reaction rates, probably not more than one order. Second, reaction 1 occurs through the strong pre-reaction complexes SO₃·H₂O or SO₃·(H₂O)₂. Binding energies of these complexes are estimated to be of 35.0 and 82.2 kJ/mol (B3LYP/3df). Thus, the kinetics of the reaction should be significantly influenced by the processes of chemical activation. Usually, the strict statistical consideration in similar systems (see for example the recent work [26]) increases the reaction rates by 1 or 2 orders of magnitude in comparison with the TST results. Therefore, we consider the obtained results as a confirmation of the conclusion made in refs 4 and 12 that the SO₃ hydration is completely described by reaction 1b. The TST results obtained at the best levels of quantum theory can be considered as a rather good approximation providing a good compromise between the detailed statistical description (e.g., RRKM − Master Equation approach) and practical tasks (mechanistic studies of reactions with multiple reaction channels). We also conclude that the

levels of theory providing the best agreement for the SO₃−H₂O system (MP2/2df) and MP2/3df//B3LYP/3df should work well also in similar systems including the SOCl₂ reactions.

SOCl₂ Hydrolysis. As evident from the results on SO₃ hydration, the B3LYP/3df level is accurate enough for making preliminary conclusions on the qualitative description of the reaction mechanism. Therefore, we used this level of theory for the preliminary calculations of the transition states of reactions of molecular SOCl₂ hydrolysis (reactions 2−6). All the transition states indicated in the above molecular reactions have been located at this level of theory except the "concerted" transition state TS4. Although many attempts to find TS4 were undertaken using the different starting geometries, it was impossible to locate the true transition structure for reaction 4. All of the structures optimized in these attempts contained two or more imaginary frequencies. The largest of these frequencies corresponded to the "proper" transition mode, i.e., to the symmetric H−O−H stretching mode leading to the transition of two hydrogen atoms from the water molecule to chlorine atoms. However, the asymmetric H−O−H stretching mode was always present, leading to the breaking of the symmetry and distortion of the transition structure. The elimination of this imaginary mode resulted always in the transition state TS1 of successive hydrolysis of two S−Cl bonds. We conclude that there is no transition state on PES of the SOCl₂ + H₂O system corresponding to the concerted mechanism and, consequently, the elementary reaction 4 is impossible.

All other transition states located for this system had the well-defined single imaginary frequency, and the visualization of the vibrational modes showed the clear movements of H, Cl, and O atoms in agreement with the corresponding reaction. The optimized geometry structures of the transition states of reactions 2−6 are shown in Figure 3 (the geometry parameters of source SOCl₂ calculated at the B3LYP/3df and MP2/2df (in parentheses) levels are: r(S−Cl), Å = 2.112(2.089); r(S−O), Å = 1.438 (1.444); ∠OSCl, degrees = 107.8(107.9); ∠ClSCl, degrees = 98.2(96.7)). For the dissociative addition (reaction (7a)), two different conformations of transition state TS9 were found distinguishing by orientation of the S=O bond relative to the S−H−OH plane. Both structures are presented in Figure 4. We found also during the modeling of reaction 7 that there was no tendency in the SOCl₂ + H₂O system to form HOCl and SOClH products. Although we did not perform a special search of
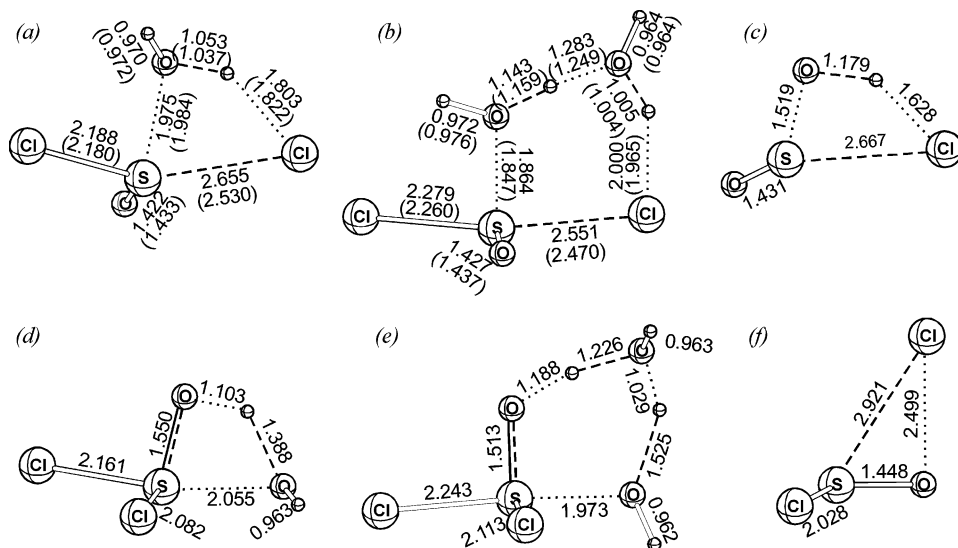

Figure 3. B3LYP/3df and MP2/2df (in parentheses) optimized structural parameters of transition states of SOCl₂ hydrolysis reactions: (a) TS2a; (b) TS2b; (c) TS3; (d) TS5a; (e) TS5b; (f) TS7.

TABLE 2: Calculated Reaction Enthalpies and Gibbs Free Energies, Energies and Imaginary Frequencies of Transition States, and Kinetic Parameters of the Possible SOCl$_2$ Hydrolysis Reactions (kJ/mol)

reaction	ΔH_r^a	ΔG_r^a	E_{tot}^b a.u.	ν_{im}^b cm^{-1}	E_a^b	$\Delta H_0^{\neq b}$	$\Delta G^{\neq b}$
Bimolecular S−Cl hydrolysis							
SOCl$_2$ + H$_2$O → [TS2a] → SOCl(OH) + HCl	−3.2	−1.2	−1470.3517527	166i	94.5	98.4	138.5
SOCl(OH) → [TS3] → SO$_2$ + HCl	−33.8	−73.2	−1009.5172494	1323i	82.6^c	63.5^c	64.3^c
Termolecular S−Cl hydrolysis							
SOCl$_2$ + 2H$_2$O → [TS2b] → SOCl(OH) + HCl + H$_2$O	−3.2	−1.2	−1546.8370999	317i	39.8	50.7	129.3
Bimolecular S=O hydrolysis							
SOCl$_2$ + H$_2$O → [TS5a] → SCl$_2$(OH)$_2$	55.1	101.7	−1470.3285900	979i	155.3	156.1	198.0
SCl$_2$(OH)$_2$ → [TS6] → SOCl(OH) + HCl	−58.3	−102.9					
Termolecular S=O hydrolysis							
SOCl$_2$ + 2 H$_2$O → [TS5b] → SCl$_2$(OH)$_2$ + H$_2$O	55.1	101.7	−1546.8173383	700i	91.7	100.5	181.1
Monomolecular chlorine shift							
SOCl$_2$ → [TS7] → Cl−S−O−Cl	188.5	186.6	−1393.8418439	436i	213.7	209.8	207.9
Cl−S−O−Cl + H$_2$O → [TS8] → SOCl(OH) + HCl	−33.8	−73.2					
Dissociative addition of H$_2$O							
SOCl$_2$ + H$_2$O → [TS9] → O=SHCl$_2$(OH), Structure 1			−1470.2638239	1302i	325.3	318.1	364.7
SOCl$_2$ + H$_2$O → [TS9] → O=SHCl$_2$(OH), Structure 2			−1470.2446321	980i	375.7	366.3	410.4

^{a} G3 calculations. ^{b} B3LYP/3df calculation. ^{c} Relative to source SOCl$_2$ and H$_2$O.
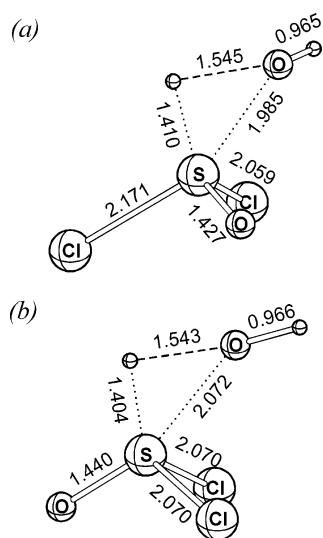

Figure 4. Two possible structures of TS9 calculated at the B3LYP/3df level. (a) Structure 1; (b) Structure 2.

corresponding transition state, the bringing of Cl and O atoms close to each another (with significant excess of energy) did not result in the straightforward formation of S−H and O−Cl bonds, probably because of their energetic unprofitableness in comparison with S−Cl or S−O structures.

Table 2 shows the calculated values of total energies of located transition states, the corresponding imaginary frequencies, and the activation energies, the energies corrected by ZPE, and the Gibbs free energies of the located transition states. To describe the driving forces of the reaction mechanisms, the reaction enthalpies and Gibbs free energies of the considered elementary processes calculated at the G3 level are also presented.

As it can be concluded from Table 2, the rate-determining steps of all the multistep processes are the initial hydrolysis of the first S−Cl (or hydration of S=O) bond. The first step of the bimolecular mechanism is characterized by a high activation energy and the Gibbs free energy (94.5 and 138.5 kJ/mol). The reaction occurring through the termolecular transition state TS2b has a lower barrier. However, in contrast with SO$_3$ hydration, the lowering of the activation barrier due to the coordination of a second water molecule is quite small, under 10 kJ/mol in comparison with 70 kJ/mol for the SO$_3$ + 2H$_2$O system. Nevertheless, the obtained activation barrier for reaction 2b has

the lowest value both of the energy and the Gibbs free energy of activation among all the molecular reactions considered here. The hydration of the S=O bond in SOCl$_2$ appears to be much slower than the S=O hydration in SO$_3$ and the S−Cl hydrolysis. This takes place for both bi- and termolecular transition states. The most unfavorable reactions are the "monomolecular" chlorine shift requiring the strong rearrangement of SOCl$_2$ to Cl−S−O−Cl structure with bivalent sulfur and the formation of the hexavalent sulfur derivative with energy of activation of more than 350 kJ/mol.

The results presented here lead to the conclusion that the most probable candidates for the molecular mechanism of hydrolysis are reactions 2a and 2b. Because the B3LYP/3df level is probably not accurate enough to provide realistic values of rate constants, additional calculations were performed at higher theory levels in order to obtain more accurate estimates of the corresponding barrier heights. The results of these calculations are presented in Table 3 together with the estimated bi- and termolecular kinetic constants.

As follows from the Table 3, improvement of the theory level has only a small effect on the calculated kinetic parameters. The only exception is the MP2/VDZ results, which give significantly lower activation energy than other methods. However, this lowering is nevertheless too small to provide the good coincidence with the experimental value. Typically, the estimated bimolecular rate constants are by 9−10 orders of magnitude lower than the observed value. The best coincidence takes place at the MP2/VDZ level. However, even in this case, the discrepancy is approximately 6 orders of magnitude. At the best optimization level (MP2/3df) the calculated rate constant for the bimolecular reaction is 10 orders of magnitude lower than the experimental value. As described above, the corresponding rate constant for the SO$_3$ + H$_2$O system obtained at the same level of theory was only two orders less than the experimental one and this discrepancy could be explained taking into account the formation of the strong complex between SO$_3$ and H$_2$O. In the case of SOCl$_2$, the binding energy of the pre-reaction complex is expected to be rather low. To validate this, the B3LYP/3df optimization of various conformations of the SOCl$_2$·H$_2$O and SOCl$_2$·(2H$_2$O) were performed. The optimized structures are shown in Figure 5, and the corresponding binding energies are given in Table 4. Among them, the most favorable conformation is the structure with the O···S coordinated water molecule and an additional O···H bond with a binding energy of only about 13.9 kJ/mol. The S···O bonded structure without

Mechanisms of SO₃ and SOCl₂ Reactions with Water

J. Phys. Chem. A, Vol. 108, No. 16, 2004 **3647**

TABLE 3: Calculated Total Energies E_{tot}, and Imaginary Frequencies ν_{im} of Transition States, Kinetic Parameters, and Rate Constants k of S−Cl Bond Hydrolysis of SOCl₂

reaction	E_{tot} a.u.	ν_{im} cm⁻¹	$E_a{}^a$ kJ mol⁻¹	$\Delta H_0{}^{\neq b}$ kJ mol⁻¹	$\Delta G^{\neq c}$ kJ mol⁻¹	k cm³ molecule⁻¹ s⁻¹
SOCl₂ + H₂O → [TS2a] → SOCl(OH) + HCl						
B3LYP/2d	−1470.3311049	271i	92.8	94.0	134.1	8.2 (−31)
B3LYP/3df	−1470.3517527	166i	94.5	98.4	138.5	1.4 (−31)
MP2/VDZ	−1468.2390598		68.6	(72.5)^d	(112.6)^d	4.7 (−27)
MP2/2df	−1468.4858618		95.2	(99.1)^d	(139.2)^d	1.0 (−31)
MP2/3df	−1468.5058003		92.5	(96.4)^d	(136.5)^d	3.1 (−31)
CCSD(T)/VDZ//MP2/VDZ	−1468.2969086		84.9	(88.8)^d	(128.9)^d	6.6 (−30)
CCSD(T)/VDZ//MP2/2df	−1468.2933697		82.0	(85.9)^d	(126.0)^d	2.1 (−29)
QCISD(T)/2df//MP2/2df	−1468.5649398		109.3	(113.2)^d	(153.3)^d	3.5 (−34)
experiment⁹						6.3 (−21)

reaction	E_{tot} a.u.	ν_{im} cm⁻¹	$E_a{}^a$ kJ mol⁻¹	$\Delta H_0{}^{\neq b}$ kJ mol⁻¹	$\Delta G^{\neq c}$ kJ mol⁻¹	cm⁶ molecule⁻¹ s⁻¹ [cm³ molecule⁻¹ s⁻¹]^e
SOCl₂ + 2H₂O → [TS2b] → SOCl(OH) + HCl + H₂O						
B3LYP/2d	−1546.8138068	467i	38.5	48.7	127.4	4.8 (−49) [2.4 (−31)]
B3LYP/3df	−1546.8370999	317i	39.8	50.7	129.3^d	2.3 (−49) [1.1 (−31)]
MP2/VDZ	−1544.829336		10.2	(21.1)^d	(99.7)^d	3.5 (−44) [1.7 (−26)]
MP2/2df	−1544.829336		33.1	(44.0)^d	(122.6)^d	3.4 (−48) [1.7 (−30)]
CCSD(T)/VDZ//MP2/VDZ	−1544.5924709		28.1	(39.0)^d	(117.6)^d	2.6 (−47) [1.3 (−29)]

^{a} Activation energy. ^{b} Zero-temperature enthalpy of activation $\Delta H_0{}^{\neq} = E_a + \text{ZPE}$. ^{c} Standard Gibbs free energy of activation. ^{d} Calculated on the basis of the B3LYP/3df frequencies and moments of inertia. ^{e} The values in square brackets are "effective bimolecular constants" k_{II} converted from termolecular rate constant by formula $k_{II} = k_{III}[\text{H}_2\text{O}]$ (where $[\text{H}_2\text{O}] = 5 \times 10^{17}$ molecules/cm³—typical experimental concentrations of water). Only k_{II} can be directly compared with experimental values for SOCl₂ hydrolysis.

TABLE 4: Calculated (B3LYP/3df) Total Energies E_{tot}, Association Energies ΔE, and Thermodynamic Parameters of the Complexes of SOCl₂ Molecule with Water (kJ/mol). BSSE Corrected Values Are Given in Parentheses

| molecular structure	E_{tot}	ΔE	$\Delta E + \text{ZPE}$	ΔH	ΔG
SOCl₂·H₂O					
Structure 1, Figure 5a	−1470.3930322	−13.9 (−11.2)	−9.1 (−6.4)	−8.4 (−5.7)	21.4 (24.1)
Structure 2, Figure 5b	−1470.3915882	−10.1 (−7.2)	−6.5 (−3.6)	−4.8 (−2.0)	20.9 (23.8)
SOCl₂·2H₂O					
Structure 1, Figure 5c	−1546.8702742	−47.3 (−41.9)	−31.9 (−26.5)	−34.3 (−28.9)	35.8 (41.2)
Structure 2, Figure 5d	−1546.8680063	−41.4 (−36.4)	−27.1 (−22.1)	−28.7 (−23.7)	38.1 (43.0)

the O···H bond (with two H···Cl contacts) is less favorable. The purely hydrogen-bonded structure S=O···H−OH is unstable and rearranged spontaneously to one of the S···O bonded complexes. The binding energy of the stable structures is believed to be too small for chemical activation of the reaction with a barrier height of 40−100 kJ/mol, and thus it cannot have any remarkable effect on the kinetics of the SOCl₂ hydrolysis.

Although the termolecular transition state has a somewhat lower activation barrier, the effect of this decrease is almost negligible. The termolecular reaction constants converted to the "effective bimolecular constants" by expression $k_{II} = k_{III}[\text{H}_2\text{O}]$ (where the H₂O concentration was taken close to the typical experimental conditions 5×10^{17} molecules/cm³) differ only by 1 order of magnitude or even less than the corresponding values obtained for the bimolecular mechanism and are also quite far from the experimental values.

On the basis of the presented results, we conclude that the fast gas-phase SOCl₂ hydrolysis cannot occur through the conventional four-membered transition state of reaction 2a and the coordination of the second water molecule, although it has some positive effect, cannot completely explain the fast hydrolysis rate observed experimentally.

Discussion

Consideration of the SO₃ hydration on the best available level of theory confirms the conclusion of ref 12 that this reaction occurs through the six-membered cyclic transition state with two coordinated water molecules. The rate constants calculated for this mechanism at the best available level of theory are in a good agreement with the experimental values.
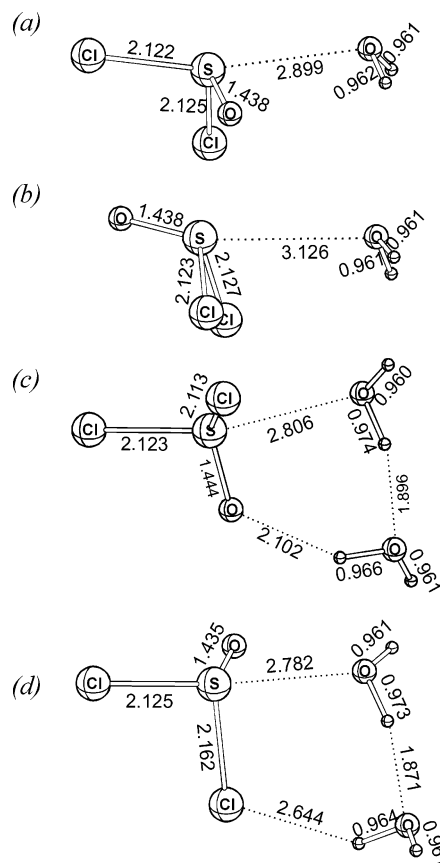

Figure 5. B3LYP/3df optimized structure of complexes SOCl₂·H₂O (a, b) and SOCl₂·2H₂O (c, d) in two different conformations.

At the same time, none of the proposed reaction mechanisms can explain the fast hydrolysis of $SOCl_2$ due to the unrealistically low calculated reaction rates. One can definitely conclude that the $SOCl_2$ hydrolysis in the gas phase cannot occur through the four-membered transition state because of the high activation barrier and the coordination of the second water molecule to this transition state (in contrast with SO_3) has a small effect on the kinetic constant.

The failure in describing the fast hydrolysis rate by molecular and radical mechanisms raises the question about the possible reasons for this result. In this context, some effects can be analyzed as a possible explanation of the obtained results:

1. The quantum chemical theory used here failed to take into account the large part of the dynamic correlation in the located transition structures (e.g., TS2a or TS2b), probably because of several second-row atoms present in the molecule. Some facts, however, speak against this explanation. First of all, no noticeable improvements were observed at the CCSD(T)/aug-cc-VTZ and MP2/3df levels. It should also be noted that, for good agreement with the experimental constants, it is necessary to lower the energy of transition states TS2a and TS2b by 40−50 kJ/mol. It is quite unlikely that the B3LYP/3df and MP2/2df calculations failed to take into account such a large part of dynamic correlation energy.

2. The wave functions of the molecular transition structures considered here have a sufficiently multireference nature and cannot be modeled by the quantum chemical methods used here. This could be true, for example, if the real transition structure would have an ion pair character, i.e., $(H_3O^+) \cdot SOCl_2 \cdot (OH^-)$, with a strongly polarized $SOCl_2$ molecule stabilizing the ionic pair. Because the OH anion has a high activity in the substitution reactions, the process

$$(H_3O^+) \cdot SOCl_2 \cdot (OH^-) \rightarrow (H_3O^+) \cdot SOCl(OH)_2 \cdot (Cl^-) \rightarrow$$
$$H_2O \cdot SOCl(OH) \cdot HCl$$
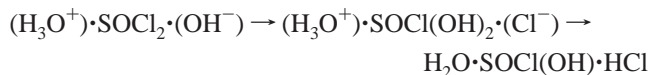
should be fast. The ion-pair wave function cannot be described correctly in the single reference approximation used in B3LYP and MP2 calculations. If the real wave function is a sufficiently multireference one, its energy cannot be described well even by the high correlated methods, e.g. by CCSD(T) or QCISD-(T).

3. Incorrect calculation of the Gibbs free energy of activation because of anharmonicity effects in the transition state structures regarding the flat and anharmonic PES of coordinated water molecules. However, it should be noted that the similar transition structure found in $SO_3 + 2H_2O$ system demonstrates no serious problems and allows concluding that the RRHO approximation works well in calculating $\Delta G^{\neq}$ of even such flexible structures. It is also possible that the conventional transition state theory does not work well for the reactions occurring through the three-molecular transition states. The results of the SO_3 hydration show that the incorrectness of TST should not be large and it is expected to gain the disagreement 1−2 orders in magnitude as as obtained for the $SO_3 + 2H_2O$ reactions.

4. Effect of the hydrogen tunneling is anomalously large in the case of $SOCl_2$ hydrolysis. To allow an increase of the rate constant by several orders of magnitude at room temperature, the activation barrier of the hydrogen transition should be extremely narrow. This is, however, not supported by the intrinsic reaction coordinate calculations. The calculated energy profiles for the H and Cl transition are shown in Figure 6. As evident from the figure, the reaction barriers have a very regular form, typical for similar reactions, and have no narrow walls.
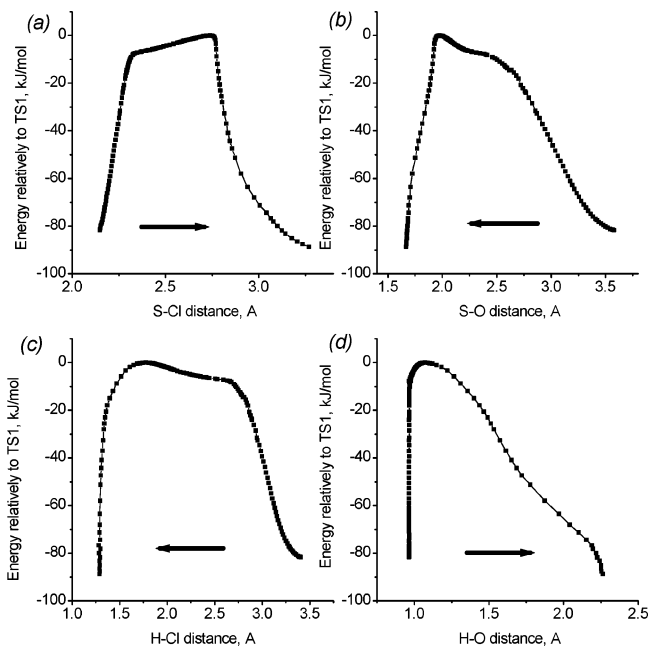

Figure 6. Calculated energy profile for the intrinsic coordinate of the reaction $SOCl_2 + H_2O \rightarrow SOCl(OH) + HCl$. Arrows mark the forward direction of reaction.

Thus, the tunneling through this wall can increase the reaction rate only slightly (not more than 1 order of magnitude as it takes place for many similar reactions), and cannot be an explanation for the anomalously high reaction rate.

5. The real reaction mechanism is sufficiently different from the proposed reactions 2−7, and the reaction occurs through the unknown but very favorable transition state. As an example of this mechanism, one can propose the ionic reactions occurring under the microsolvation conditions in the gas phase. Probably, the hydrolysis process is also catalyzed by third-side molecules present in the reaction mixture. Moreover, the possible mechanism can also be connected to the many-molecular water clusters present in the gas phase. Because of cooperative effects, the state of water molecules at the "surface" of the many-molecular cluster (consisting of several tens of molecules) can be much more strained than in the isolated H_2O molecules but also in the water dimers and trimers. Probably, the reaction with such "cooperatively activated" molecules can be significantly easier than the reaction in the gas phase.

It is also not implausible that the $SOCl_2$ hydrolysis can occur through the free-radical chain reactions initiated by Cl radicals formed from any unstable compounds. Probably, this radical mechanism involves also the reactions of oxygen or nitrogen molecules, which were present in the reaction mixture in a large amount.[9]

Although the last two explanations (a participation of large size or charged clusters and radical chain mechanism) seem to be well-founded, none from the above assumptions can be considered as most plausible. All of the above assumptions require an additional verification and, thus, the mechanism of gas-phase $SOCl_2$ hydrolysis still remains a problem for modern quantum chemistry. It should also be noted that the system considered here is not the only reaction of the inorganic halogen-containing compounds with a surprisingly high reaction rate. Another example, which was also described recently, is the gas-phase reaction of $SiCl_4$ with water at 290−400 K. The many features of this process (high reaction rate, second-order reaction for water, negative temperature dependence,[20,21] and difficulties in quantum chemical description of this reaction[19]) make it

Mechanisms of SO$_3$ and SOCl$_2$ Reactions with Water

J. Phys. Chem. A, Vol. 108, No. 16, 2004 **3649**

similar to the hydrolysis of SOCl$_2$. Probably, the similar behavior is also attributed to another halogen derivative of silicon—SiF$_4$ as it can be concluded from the fast changes in FTIR spectra of the gas-phase SiF$_4$/H$_2$O mixtures reported in our recent preliminary study of this system.[27]

On the basis of the results presented here, we can conclude that the chemistry of halogen derivatives of second-row elements and, in particular, the mechanisms of their gas-phase hydrolysis is an intriguing problem which is definitely a challenge for modern physical chemistry, requiring additional efforts for the correct description.

Supporting Information Available: Cartesian coordinates of transition states and complexes optimized at the B3LYP/3df (Tables S1−S14), MP2/2df (Tables S15−S18), and MP2/3df (Table S19) levels. This material is available free of charge via the Internet at http://pubs.acs.org.

References and Notes

(1) Seeley, J. V.; Jayne, J. T.; Molina, M. J. *Int. J. Chem. Kinet.* **1993**, *25*, 571; Seeley, J. V.; Jayne, J. T.; Molina, M. J. *J. Phys. Chem.* **1996**, *100*, 4019.

(2) Kolb, C. E.; Jayne, J. T.; Worsnop, D. R.; Molina, M.; Meads, R. F.; Viggiano, A. A. *J. Am. Chem. Soc.* **1994**, *116*, 10314.

(3) Lovejoy, E. R.; Hanson, D. R. *J. Phys. Chem.* **1996**, *100*, 4459.

(4) Jayne, J. T.; Pöschl, U.; Chen, Y.; Dai, D.; Molina, L. T.; Worsnop, D. R.; Kolb, C. E.; Molina, J. T. *J. Phys. Chem. A* **1997**, *101*, 10000.

(5) Castleman, A. W.; Davis, R. E.; Munkelwitz, H. R.; Tang, I. N.; Wood, W. P. *Int. J. Chem. Kinet. Symp.* **1975**, *1*, 629.

(6) Wang, X.; Jin, Y. G.; Suto, M.; Lee, L. C. *J. Chem. Phys.* **1988**, *89*, 4853.

(7) Reiner, T. H.; Arnold, F. *Geophys. Res. Lett.* **1993**, *20*, 2659.

(8) Reiner, T. H.; Arnold, F. *J. Chem Phys.* **1994**, *101*, 7399.

(9) Johnson, T. J.; Disselkamp, R. S.; Su, Y.-F.; Fellows, R. J.; Alexander, M. L.; Driver, C. J. *J. Phys. Chem. A* **2003**, *107*, 6183.

(10) Chen, T. S.; Moore-Plummer, P. L. *J. Phys. Chem.* **1985**, *89*, 3689.

(11) Hofmann, M.; Schleyer, P. *J. Am. Chem. Soc.* **1994**, *116*, 4947.

(12) Morokuma, K.; Muguruma, C. *J. Am. Chem. Soc.* **1994**, *116*, 10316.

(13) Vincent, M. A.; Palmer, I. J.; Hillier, I. H.; Akhmatskaya, E. *J. Am. Chem. Soc.* **1998**, *120*, 3431.

(14) Kudo, T.; Gordon, M. S. *J. Am. Chem. Soc.* **1998**, *120*, 11432.

(15) Kudo, T.; Gordon, M. S. *J. Phys. Chem. A* **2000**, *104*, 4058.

(16) Ignatyev, I. S.; Partal, F.; López González, J. J. *Chem. Phys. Lett.* **2003**, *368*, 616.

(17) Okumoto, S.; Fujita, N.; Yamabe, S. *J. Phys. Chem. A* **1998**, *102*, 3991.

(18) Lewis, M.; Glaser, R. *J. Phys. Chem. A* **2003**, *107*, 6814.

(19) Ignatov, S. K.; Sennikov, P. G.; Razuvaev, A. G.; Chuprov, L. A.; Schrems, O.; Ault, B. S. *J. Phys. Chem. A* **2003**, *107*, 8705.

(20) Sagitova, V. G.; Chernyak, V. I. *Zhurn. Obsh. Khimii* **1983**, *53* (2), 397.

(21) Kochubei, V. F. *Kinetika i Kataliz* **1997**, *38* (2), 234.

(22) Frisch, M. J.; Trucks, G. W.; Schlegel, H. B.; Scuseria, G. E.; Robb, M. A.; Cheeseman, J. R.; Zakrzewski, V. G.; Montgomery, J. A., Jr.; Stratmann, R. E.; Burant, J. C.; Dapprich, S.; Millam, J. M.; Daniels, A D.; Kudin, K. N.; Strain, M. C.; Farkas, O.; Tomasi, J.; Barone, V.; Cossi, M.; Cammi, R.; Mennucci, B.; Pomelli, C.; Adamo, C.; Clifford, S.; Ochterski, J.; Petersson, G. A.; Ayala, P. Y.; Cui, Q.; Morokuma, K.; Malick, D. K.; Rabuck, A. D.; Raghavachari, K.; Foresman, J. B.; Cioslowski, J.; Ortiz, J. V.; Stefanov, B. B.; Liu, G.; Liashenko, A.; Piskorz, P.; Komaromi, I.; Gomperts, R.; Martin, R. L.; Fox, D. J.; Keith, T.; Al-Laham, M. A.; Peng, C. Y.; Nanayakkara. A.; Gonzalez, C.; Challacombe, M.; Gill, P. M. W.; Johnson, B. G.; Chen, W.; Wong, M. W.; Andres, J. L.; Head-Gordon, M.; Replogle, E. S.; Pople, J. A. *Gaussian 98*, revision A.3; Gaussian, Inc.: Pittsburgh, PA, 1998.

(23) Curtiss, L. A.; Raghavachari, K.; Redfern, P. C.; Rassolov, V.; Pople, J. A. *J. Chem. Phys.* **1998**, *109*, 7764. Curtiss, L. A.; Redfern, P. C.; Raghavachari, K.; Rassolov, V.; Pople, J. A. *J. Chem. Phys.* **1999**, *110*, 4703.

(24) Pitzer, K. S.; Gwinn, W. D. *J. Chem. Phys.* **1942**, *10*, 428. Pitzer, K. S. *J. Chem. Phys.* **1946**, *14*, 239.

(25) Ignatov, S. K.; Razuvaev, A. G.; Sennikov, P. G.; Nabviev, S. S. *Proc. of VIII Joint Int. Symp. "Atmospheric and ocean optics. Atmospheric physics."* June 25−29, 2001, Irkutsk. 93.

(26) Liu, J.; Li, Z.; Dai, Z.; Xuang, X.; Sun, C. *J. Phys. Chem. A* **2003**, *107*, 6231.

(27) Ignatov, S. K.; Sennikov, P. G.; Razuvaev, A. G.; Chuprov L. A. *Russ. Chem. Bull.* **2003**, *4*, 837.